1990

COSEISMIC STRESS CHANGES INDUCED BY THE 1989 LOMA PRIETA, CALIFORNIA EARTHQUAKE

Andrew J. Michael
U.S. Geological Survey

William L. Ellsworth
U.S. Geological Survey

David H. Oppenheimer
U.S. Geological Survey

GEOPHYSICAL RESEARCH LETTERS, VOL. 17, NO. 9, PAGES 1441-1444, AUGUST 1990

COSEISMIC STRESS CHANGES INDUCED BY THE 1989 LOMA PRIETA, CALIFORNIA EARTHQUAKE

Andrew J. Michael William L. Ellsworth David H. Oppenheimer

U.S. Geological Survey, Menlo Park, California

Abstract. Earthquake focal mechanisms from before and after the 1989 Loma Prieta, California earthquake are used to infer the coseismic stress change. Before the main shock, most earthquakes correspond to right lateral slip on planes sub-parallel to the San Andreas fault, and imply a generally N-S most compressional stress axis and a vertical intermediate stress axis. Aftershocks within the main shock rupture zone, however, display almost every style and orientation of faulting, implying an extremely heterogeneous stress field. This suggests that the main shock relieved most, if not all, of the shear stress acting on its fault plane. Aftershocks that lie on the perimeter of the rupture agree with spatially uniform stress states, but only when considered in three groups: north, south, and above the main shock rupture area. In each of these areas the stress state may reflect stress transfer by the main shock.

Introduction

In this paper we explore the implications of the surprisingly diverse collection of focal mechanism orientations observed in the aftershock sequence of the 1989 M_S 7.1 Loma Prieta earthquake for the state of stress acting on the fault and for the stress drop of the main shock. Unlike typical San Andreas fault system earthquake sequences where the aftershocks are very similar in both their locations and focal mechanisms to the prior activity, the Loma Prieta aftershocks bear little resemblance to either the main shock or background activity (Dietz and Ellsworth, 1990; Olson and Lindh, 1990; and Oppenheimer, 1990).

Before the main shock most earthquakes are right lateral slip on the creeping segment of the San Andreas fault and the Sargent fault (Figure 1), but after both the locations and the mechanisms of the earthquakes changed dramatically. In particular, within the central part of the aftershock zone where the main shock rupture occurred almost every type of focal mechanism can be found (Figure 4 in Oppenheimer, 1990), suggesting a very heterogeneous stress state, in sharp contrast to the relative simplicity of the prior seismicity.

The apparent dissimilarity between aftershock mechanisms is so strong that it suggests a post-earthquake stress field with little resemblance to stresses released in the main shock. We examine this possibility by using both forward modeling and a stress tensor inversion. While concentrating on the stress effects of the main shock, we acknowledge that other mechanisms (e.g. pore fluid effects or rigid block rotations) could play a role in creating the observed patterns.

Paper number 90GL01600
0094-8276/90/90GL-01600$03.00

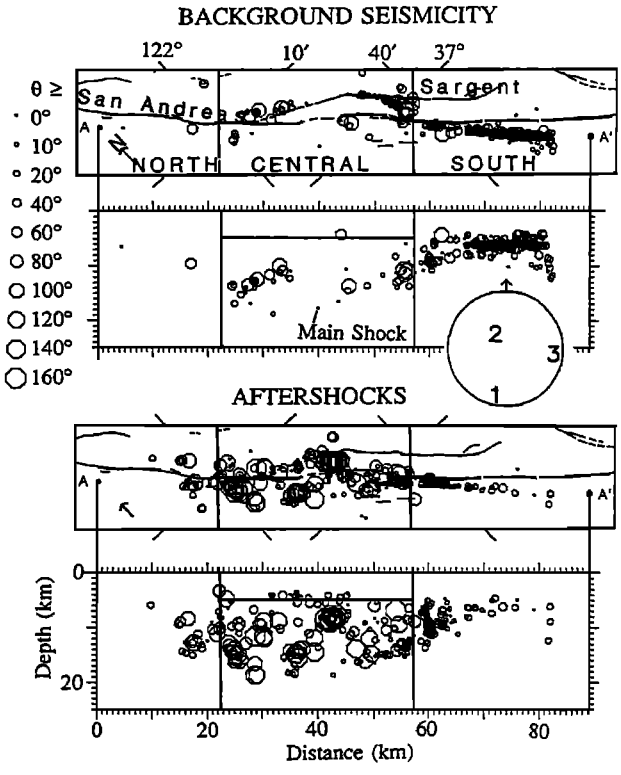

Fig. 1. Map and cross sections of background seismicity and aftershocks with symbol size scaled to the θ with respect to the stress tensor that perfectly fits the main shock and minimizes θ averaged over the background seismicity (shown on equal area stereonet, $\phi = 0.27$). The θ is the minimum β for the two possible fault planes where β is the angle between the observed slip direction and shear stress imposed by a stress tensor.

Data

We relocated the background seismicity and computed fault plane solutions such that the results are comparable to Oppenheimer's (1990) analysis of the aftershocks. After removing poor solutions and events shallower than 3km (due to poorly constrained take-off angles), the data set includes 304 prior events, M_d 0.9 to 5.2, from June 1969 to September 1989, and 350 aftershocks, M_d 0.9 to 4.5, from 30 minutes after the main shock on October 18, 1989 to November 30, 1989. On average 36 stations that are well distributed on the focal sphere were used to determine each fault plane solution. The mean standard deviation in strike, dip, and rake, as estimated from the data, is 13°.

Forward Method and Results

We assume that earthquakes relax an unknown fraction of the shear stress acting on the fault plane. We also assume that on average the slip vector is parallel to this applied shear stress and at a minimum the angle between the shear stress and the slip vector is <90°. Under these assumptions it is straightforward to compare the observed slip vectors with an assumed state of stress, and we shall use the angular error between the shear stress and the slip vector, β, as a measure of the agreement.

We wish to determine if the aftershock focal mechanisms agree with the spatially uniform stress field that best explains the background seismicity and perfectly fits the main shock. To avoid having to select which nodal plane is the fault plane we define a new misfit criterion, θ, to be the minimum β for the two possible fault planes (similar to Gephart and Forsyth, 1984) and seek to minimize the sum of θ over the background seismicity. This results in a stress field and misfits shown in Figure 1. Except for a few events near the center of the region, this tensor fits the background seismicity well with $\overline{\theta} = 23°$ (top, Figure 1). The aftershocks, however, are poorly explained by this tensor ($\overline{\theta} = 42°$). The largest misfits approach 180° and concentrate in the center of the region (bottom, Figure 1). These results suggest a coseismic change in the stress field, that is greatest in the center of the region.

Inverse Method and Results

To determine the nature of the coseismic change we solve a formal inverse problem for a state of stress consistent with the data for the background seismicity and aftershocks separately and compare the results. We use the method of Michael (1987a and 1987b) to determine the spatially uniform component of the deviatoric stress field. Tests with subsets of our data show that the results are robust, with respect to the confidence limits, for data sets with 15 or more events. From the focal mechanism data we can determine only the relative magnitudes of the deviatoric stress tensor, which can be represented by the orientations of the three principal axes and the quantity $\phi = (S_2 - S_3)/(S_1 - S_3)$, where S_1, S_2, and S_3 are the three principal stresses ordered from most compressional to most tensional (Angelier, 1979). No weighting by magnitude is used because there is no evidence that the stress field determined is dependent on the magnitudes of the events used; indeed, Michael (1987b) demonstrated that the opposite is true at Coalinga.

To apply this method to fault plane solutions we must select one nodal plane as the fault plane and estimate our confidence in this choice. While the seismicity is on a variety of structures, most strike NW-SE (Dietz and Ellsworth, 1990; Olson and Lindh, 1990). Consequently, we choose the nodal plane that is closer to a NW-SE vertical plane as our guess of the correct plane. We also assume an error rate on the fault plane picks of 50%, the greatest it can be if the true planes are oriented randomly to our assumption, when assessing the confidence limits on the inverse solution. Overestimating the error rate will increase the size of the confidence regions preventing us from overestimating the resolution.

When the stress field varies with position, A. Michael (1990, submitted manuscript) found that recovery of the uniform component of the stress field diminishes as the amount of heterogeneity increases. Using the second invariant of the deviatoric stress tensor (e.g. Jaeger, 1971) as a measure of size, that study showed that if the mean size of the spatially variable component of the stress field is larger than the size of the uniform stress component, the inversion is unlikely to recover the correct answer within the 95% confidence limits. The synthetic control study also showed that the amount of heterogeneity in the stress field could be characterized by the average misfit between the observed and predicted slip directions ($\overline{\beta}$). For focal mechanism data with errors of 13°, $\overline{\beta} \simeq 40°$ when the spatially uniform and variable parts of the stress field have equal size. If $\overline{\beta}$>40°, we will interpret the inversion results to imply a spatially heterogeneous state of stress. The simulations suggest that when the spatially averaged stress vanishes $\overline{\beta}$ will be about 65°.

Given the results of the forward modeling, we divide the region into four volumes, based on the inferred extent of the main shock rupture (Dietz and Ellsworth, 1990). The central zone is presumed to contain the rupture and the north and south zones flank it. The central zone was further divided into two depth intervals with a boundary at 5 km, to correspond to the upper extent of faulting (Lisowski et al., 1990). In each of these volumes the background focal mechanisms and aftershock focal mechanisms were inverted separately to determine the stress field for that volume and time interval.

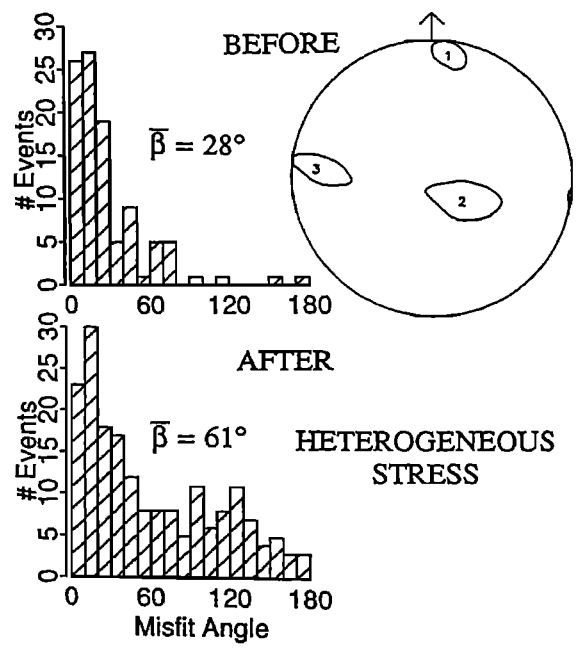

Fig. 2. Stress inversion results for the deep central region before and after the main shock. The histograms show the distribution of β for the data with respect to the stress tensor determined by the stress inversion. The equal area stereonet shows the stress axes and their 95% confidence limits. Before the main shock $\phi = 0.39$ with 95% confidence limits of (0.13, 0.48).

In the deep central zone the stress field before the main shock is relatively uniform ($\bar{\beta} = 28°$) with S_2 vertical and S_1 oriented N 8° E (Figure 2). Although this stress tensor fits the main shock poorly, with $\beta_{\text{main shock}} = 44°$, another within its 95% confidence limits fits the main shock to within 25°, which is smaller than $\bar{\beta}$. The most we can conclude is that the stress inversion result from the prior activity is not inconsistent with the main shock. The aftershocks have $\bar{\beta} = 61°$ in the deep interval and a large number of them have $\beta > 90°$ (Figure 2). As $\bar{\beta} > 40°$ we do not show the inversion's solution because the true stress tensor is unlikely to be within its 95% confidence regions; however, the distribution of $\bar{\beta}$ is displayed because there are no stress tensors that would better fit the data. Thus, for aftershocks within the inferred main shock rupture area the homogeneous component of the stress tensor is smaller than its variability. Just above the main shock rupture, there are insufficient data to determine the pre-main shock stress field. The aftershocks in the shallow interval have $\bar{\beta} = 21°$ and a homogeneous stress field with S_3 vertical and S_1 oriented N 11° E (Figure 3) fits the data.

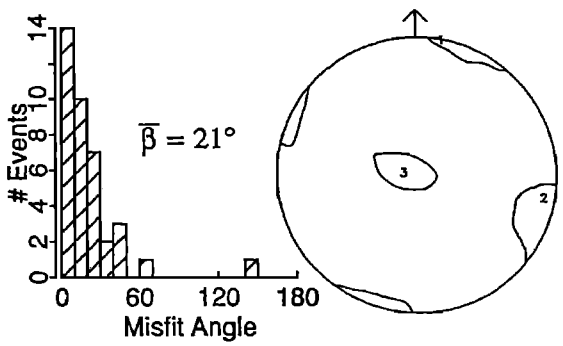

Fig. 3. Stress inversion results for the shallow central region. There are too few data to invert before the main shock. For the aftershocks $\phi = 0.55$ (0.16, 0.73). See Figure 2 for details.

In the north zone there are insufficient data to determine the stress field before the main shock. The aftershocks fit a uniform stress ($\bar{\beta} = 18°$), with S_2 or S_3 vertical and S_1 trending N 29° E, almost normal to the San Andreas fault (Figure 4).

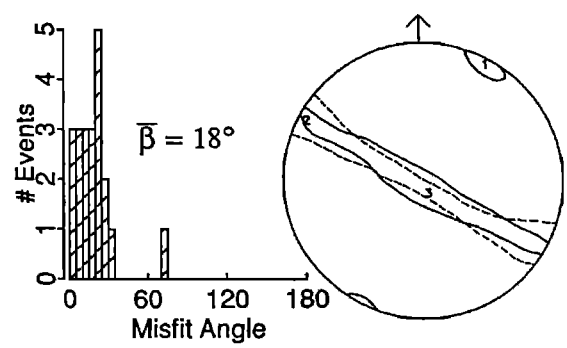

Fig. 4. Stress inversion results for the north region. There are too few data to invert before the main shock. For the aftershocks $\phi = 0.20$ (0.00, 0.44). See Figure 2 for details.

The south zone contains most of the prior seismicity; it shows a stress state that is relatively uniform ($\bar{\beta} = 21°$) with S_2 vertical and S_1 oriented N-S. After the main shock S_1 trends N 9° E with $\bar{\beta} = 14°$ (Figure 5). While the before and after stress states are distinct in a statistical sense, we discount the importance of this modest rotation (9°), given the difficulties in constructing focal mechanisms in the south zone (Oppenheimer, 1990).

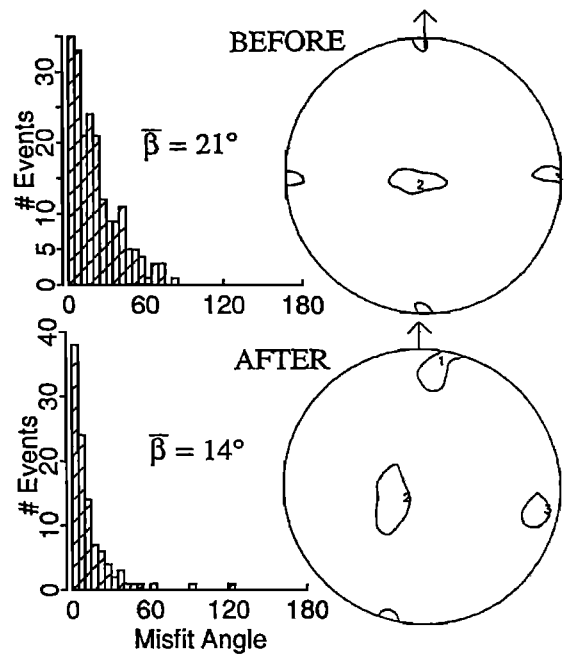

Fig. 5. Stress inversion results for the south region. For before $\phi = 0.39$ (0.18, 0.42). For after $\phi = 0.57$ (0.37, 0.85). See Figure 2 for details.

We interpret the differences and similarities between the stress states before and after the main shock to be a coseismic temporal change in stress despite the spatial changes in the hypocenters for two reasons. First, within the background seismicity, we can find no evidence for spatial variations in stress orientations. Second, the main shock is an obvious source for a temporal change.

Discussion

Before the Loma Prieta earthquake most earthquakes in the region correspond to the release of shear stress in an environment dominated by north-south compression. This same stress field also fits the aftershocks in the southern part of the zone. Within the northern and shallow central parts of the zone the aftershocks release compression oriented at a high angle to the San Andreas fault. Many of the aftershocks have a steeply-dipping nodal plane that parallels the fault, but release almost no dextral shear. Too few events preceded the main shock in these two areas to permit a comparison of the pre- and post-event stress fields.

Within the main shock rupture area no spatially invariant stress tensor can satisfy the slip vectors of most aftershocks, and many have slip vectors oriented >90° from

the mean applied shear traction. The aftershock focal mechanisms demand a highly heterogeneous stress field. While this heterogeneity could include both spatial and temporal components, diverse and discordant focal mechanisms occur throughout the first six weeks of the sequence. As few of the aftershocks either resemble the main shock or correspond to release of the same stress field, we suggest that the main shock released most, if not all, of the traction acting on its fault plane. In other words, the main shock stress drop appears to be nearly total.

The pattern of stress release in the aftershock sequence qualitatively corresponds with the stress changes expected around an elastic dislocation, but only if the stress change is a large fraction of the pre-stress. Dislocation stresses are largest near discontinuities in the dislocation pattern; these occur near the edges of the rupture and within the rupture if it contains variations in slip magnitude and orientation (Segall and Pollard, 1980). Thus we would expect the greatest heterogeneities in the stress field to be found in the main shock rupture area, as is observed. Outside of the rupture, a dislocation transfers shear stresses of the same sense as it released to the continuation of its fault plane. Geodetic models of the main shock (Lisowski et al., 1990) suggest predominantly strike slip motion near the southern termination of rupture, so we would expect it to transfer dextral shear to the fault farther to the south. As N-S compression was the pre-main shock stress state, the dislocation stress would reinforce the pre-stress. To the north the same main shock model suggests a larger thrust component. This might explain the absence of right lateral shear on the San Andreas fault to the north and above the rupture during the aftershock sequence.

While the complex pattern of focal mechanisms in the central zone argues for nearly complete stress release in the main shock, placing a numerical value on the stress is highly model dependent. At one extreme a uniform dislocation, as used in the geodetic modeling, corresponds to a stress drop of about 2.5 MPa, whereas a heterogeneous model consistent with the main shock ground motion in the near field implies localized stress drops of 100MPa or more (A. McGarr, personal communication, 1990; McGarr, 1984). A highly irregular slip distribution on the fault plane could create sufficient variations in the stress field to explain the diverse aftershock mechanisms, although this remains to be demonstrated.

Conclusions

Fault plane solutions of the Loma Prieta sequence provide us with evidence of how the earthquake altered the state of stress at seismogenic depths. The post-earthquake stress field is complicated and will require further study to understand it in detail. One basic pattern is clear, however, and we believe it will be unchanged by further study. The main shock left the stress field within the rupture area in a spatially heterogeneous state. As most aftershocks near the rupture have focal mechanisms that disagree with the pre-stress, we suggest that the main shock released most of the traction acting on the fault plane resulting in an almost total stress drop earthquake.

Acknowledgements. We thank Dave Hill, Art McGarr, and Paul Reasenberg for critical reviews.

References

Angelier, J., Determination of the mean principal directions of stresses for a given fault population, *Tectonophysics, 56,* T17-T26, 1979.

Dietz, L.D., and W.L. Ellsworth, The October 17, 1989 Loma Prieta, California, earthquake and its aftershocks: geometry of the sequence from high-resolution locations, *Geophys. Res. Lett.*, in press, 1990.

Gephart, J.W., and D. W. Forsyth, An improved method for determining the regional stress tensor using earthquake focal mechanism data: Application to the San Fernando earthquake sequence, *J. Geophys. Res., 89,* 9305-9320, 1984.

Jaeger, J.C., *Elasticity, Fracture and Flow: With Engineering and Geological Applications*, 268 pp., Metheun and Co. Ltd., 1971.

Lisowski, M., W.H. Prescott, J.C. Savage and M.J. Johnston, Geodetic estimate of coseismic slip during the 1989 Loma Prieta, California, earthquake, *Geophys. Res. Lett.*, in press, 1990.

McGarr, A., Scaling of ground motion parameters, state of stress and focal depth, *J. Geophys. Res., 89,* 6969-6979, 1984

Michael, A.J., The use of focal mechanisms to determine stress: A control study, *J. Geophys. Res., 92,* 357-368, 1987a.

Michael, A.J., Stress rotation during the Coalinga aftershock sequence, *J. Geophys. Res., 92,* 7963-7979, 1987b.

Olson, J. and A. Lindh, Seismicity preceding the Loma Prieta earthquake (abstract), *EOS Trans AGU, 71,* 289, 1990.

Oppenheimer, D.H., Aftershock slip behavior of the 1989 Loma Prieta, California earthquake, *Geophys. Res. Lett.,*, in press 1990.

Segall, P., and D.D. Pollard, Mechanics of discontinuous faults, *J. Geophys. Res., 85,* 4337-4350, 1980.

W.L. Ellsworth, A.J. Michael, and D.H. Oppenheimer, Branch of Seismology, U.S. Geological Survey, MS/977, 345 Middlefield Road, Menlo Park, CA 94025

(Received March 6, 1990;
revised July 3, 1900;
accepted July 3, 1900.)